Anal. Chem. **2010,** *82,* 1698–1704

Visualizing the Lower Critical Solution Temperature Phase Transition of Individual Poly(Nipam)-Based Hydrogel Particles Using Near-Infrared Multispectral Imaging Microscopy

Irena Mejac,[†] Hye-Hun Park,[‡] William W. Bryan,[‡] T. Randall Lee,[‡] and Chieu D. Tran*,[†]

Department of Chemistry, Marquette University, P.O. Box 1881, Milwaukee, Wisconsin 53201, Department of Chemistry, University of Houston, 4800 Calhoun Road, Houston, Texas 77204

This manuscript reports the use of near-infrared multispectral imaging (NIR-MSI) microscopy to provide the first direct observation and spectral measurement of individual poly(*n*-isopropylacrylamide-*co*-acrylic acid) (NIPAM-*co*-AAc) hydrogel particles. The high sensitivity and high spatial resolution (~0.9 μm/pixel) of the NIR-MSI microscope, coupled with its ability to measure images and spectra directly and simultaneously, allows the unprecedented in situ monitoring of the size, morphology, and spectroscopic properties of individual hydrogel particles, which respond strongly to external stimuli (e.g., changes in temperature and/or pH). Importantly, this novel technique allows, for the first time, the direct measurement of the lower critical solution temperature (LCST) phase transition of individual hydrogel particles rather than that of a collection of hydrogel particles. Furthermore, NIR-MSI measurements reveal that the LCST value is unique for each individual hydrogel particle, depending strongly on particle size, with larger particles exhibiting higher LCST values.

Water-soluble hydrogel polymers such as poly(*n*-isopropylacrylamide) poly(NIPAM) have drawn the interest of scientists and engineers due to their unique responsive behavior to external stimuli (e.g., temperature and pH).[1] Most notably, samples of poly(NIPAM) in aqueous solution rapidly undergo volume transitions that depend on the lower critical solution temperature (LCST), which is influenced by chemical and/or physical parameters.[2] Poly(NIPAM) microstructures in aqueous solution are hydrophilic and swollen below the LCST but become hydrophobic and collapsed above the LCST.[3,4] Importantly, poly(NIPAM) and particularly its copolymer with acrylic acid, poly(NIPAM-*co*-AAc), exhibit LCST transitions near physiologic temperature, which has motivated research efforts directed toward various biomedical applications, including those involving drug delivery and microfluidics.[1,5,6]

On the basis of studies of poly(NIPAM) using various experimental techniques (i.e., calorimetry, NMR, fluorescence, dynamic light scattering, neutron scattering, and dielectric relaxation), several groups have proposed mechanisms regarding the miscibility of poly(NIPAM) in water.[7−14] Perhaps the most widely accepted view is that the miscibility arises largely from hydrogen bonding between the amide groups and water; in addition, it is assumed that the water molecules are ordered around the hydrophobic isopropyl groups. Studies concerning the LCST liquid−liquid miscibility behavior of poly(NIPAM) have revealed that the macroscopic liquid−liquid phase separation of these polymer solutions is accompanied by changes in the hydration of the polymer chains.[2,4] In solution, the polymer chains become dehydrated with increasing temperature, and attractive interactions between hydrophobic moieties prevail, leading to collapse of the polymer network at sufficiently dilute concentrations.

Given that the results of these studies can only partially rationalize the miscibility behavior of poly(NIPAM), further investigations are needed to develop a comprehensive model. In particular, LCST studies involving poly(NIPAM) hydrogel particles are plagued by variations in particle size, morphology, and stability. Specifically, the polydispersity of hydrogel particles leads to strong inhomogeneities in their spectroscopic response and hinders the comparison of data obtained from independent experiments and also data obtained from experiment and computation. A comprehensive rationalization of the LCST behavior of poly(NIPAM) hydrogel particles is needed to exploit these polymers fully in

* To whom correspondence should be addressed. E-mail: chieu.tran@marquette.edu.

[†] Marquette University.

[‡] University of Houston.

(1) Peppas, N. A.; Huang, Y.; Torres-Lugo, M.; Ward, J. H.; Zhang, J. *Annu. Rev. Biomed. Eng.* **2000**, *2*, 9–29.
(2) Hirotsu, S.; Hirokawa, Y.; Tanaka, T. *J. Chem. Phys.* **1987**, *87*, 1392–1395.
(3) Hirokawa, Y.; Tanaka, T. *J. Chem. Phys.* **1984**, *81*, 6379–6380.
(4) Li, Y.; Tanaka, T. *Annu. Rev. Mater. Sci.* **1992**, *22*, 243–277.
(5) Bromberg, L.; Temchenko, M.; Alakhov, V.; Hatton, T. A. *Langmuir* **2005**, *21*, 1590–1598.
(6) Beebe, D. J.; Moore, J. S.; Bauer, J. M.; Yu, Q.; Liu, R. H.; Devadoss, C.; Jo, B.-H. *Nature* **2000**, *404*, 588–590.
(7) Kawasaki, H.; Sasaki, S.; Maeda, H. *Langmuir* **1998**, *14*, 773–776.
(8) Shibayama, M.; Mizutani, S.; Nomura, S. *Macromolecules* **1996**, *29*, 2019–2025.
(9) Zhou, S.; Chu, B. *J. Phys. Chem. B* **1998**, *102*, 1364–1368.
(10) Snowden, M. J.; Chowdhry, B. Z.; Vincent, B.; Morris, G. E. *J. Chem. Soc., Faraday Trans.* **1996**, *92*, 5013–5016.
(11) Lamanna, R.; Sobolev, A. P.; Masci, G.; Bontempo, D.; Crescenzi, V.; Segre, A. L. *Polym. Prepr.* **2003**, *44*, 406–407.
(12) Datta, A.; Das, S.; Mandal, D.; Pal, S.; Bhattacharyya, K. *Langmuir* **1997**, *13*, 6922–6926.
(13) Iwai, K.; Hanasaki, K.; Yamamoto, M. *J. Lumin.* **2000**, *87−89*, 1289–1291.
(14) Masci, G.; Cametti, C. *J. Phys. Chem. B* **2009**, *113*, 11421–11428.

10.1021/ac902099d
Published on Web 01/28/2010

practical applications. Consequently, the development of a new technique that is capable of measuring the spectroscopic properties of single hydrogel particles is urgently needed. The near-infrared multispectral imaging (NIR-MSI) microscope based on an acousto-optic tunable filter (AOTF), which was developed recently in our group, with its unique features is particularly suited for this task.[15−20]

Unlike conventional imaging techniques that collect a single image using either monochromatic or multiwavelength light for illumination, the NIR-MSI microscope collects a series of several thousand images, each at a specific wavelength.[15−21] Moreover, it measures the absorption spectra of a sample not at a single position, as is the case for a conventional spectrophotometer, but simultaneously at many different positions within a sample (using a focal plane array detector rather than a single channel detector). Importantly, the chemical composition and structure at different positions within a sample can be derived from such images. Given its high sensitivity and high spatial resolution (single pixel resolution with approximately micrometer spatial resolution and $\sim 10^{-4}$ absorbance unit) and rapid temporal resolution (milliseconds), this imaging technique offers unprecedented opportunities in imaging, including a detailed investigation of the LCST transitions of individual poly(NIPAM)-based hydrogel particles.[15−20]

This manuscript describes our initial investigation of the simultaneous imaging and NIR spectral measurement of discrete poly(NIPAM-*co*-AAc) hydrogel particles. In this investigation, we sought to (1) develop novel synthetic methods to prepare large hydrogel particles with diameters >1 μm, (2) observe and characterize individual hydrogel particles using NIR-MSI, (3) investigate the effect of temperature variation on the spectroscopic and spatial (volume) properties of individual hydrogel particles to determine LCST values of individual hydrogel particles, and (4) determine the structural effects on the LCST values of individual hydrogel particles.

EXPERIMENTAL SECTION

Materials. Deuterium oxide (99.9%) was obtained from Cambridge Isotope Laboratories, Inc. (Andover, MA); acetamide (99%) and glacial acetic acid (99.7+ %) were purchased from Sigma-Aldrich (Milwaukee, WI).

Synthesis of Poly(NIPAM-*co*-AAc) Hydrogel Particles. These particles were synthesized using procedures adopted from the literature.[22,23,21] In a typical reaction, *n*-isopropylacrylamide (NIPAM) with acrylic acid (AAc) (95:5, w/w), and cross-linker *N,N*′-methylenebisacrylamide (BIS) (NIPAM/BIS, 90:10 w/w) were dissolved in purified Milli-Q water. The solution was purged with argon for 1 h and heated to 70 °C. Ammonium persulfate (APS) was rapidly injected into the solution to initiate the polymerization, and the reaction was allowed to proceed for 5 to 6 h. After cooling, the solution was gravity filtered through qualitative filter paper to remove impurities and/or aggregated particles. Notably, the average diameter of the particles produced using this method can be increased in a systematic manner by increasing the concentration of BIS.

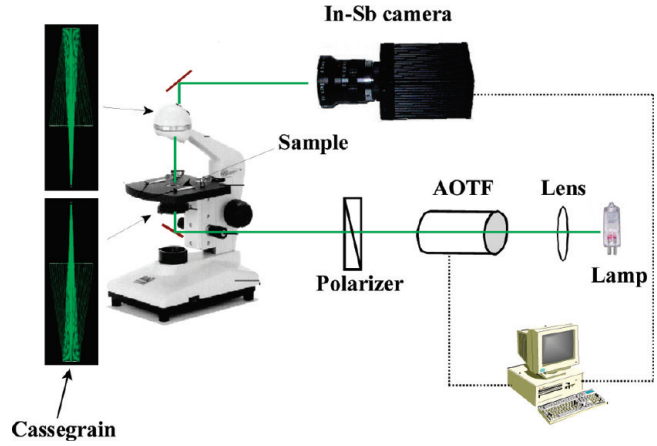

Figure 1. Schematic diagram of the near-infrared (NIR) multispectral imaging (MSI) system.

Instrumentation. A detailed description of our AOTF-based NIR multispectral imaging microscope (Figure 1) is available in the literature.[15−20] To eliminate possible aberrations in the NIR region, the focusing microscopic lenses were replaced in the present study by a pair of 0.58 N.A. 15× reflecting Cassegrains. Images recorded by the NIR camera were collected and transferred to a PC by a frame grabber. To control the imaging microscope and to facilitate frame grabbing, saving, and processing of the images, a program written in C++ language was utilized. Three-dimensional (3-D) images were calculated from recorded images using publicly available software (National Institutes of Health, ImageJ program). Unless otherwise stated, the exposure time of the camera was set at 1.0 ms. Under this condition, it took 560 ms to record an image at a specific wavelength. On the basis of methods described in our previous studies[20] and using a gold U.S. Air Force resolution target as a standard, the spatial resolution of this NIR multispectral imaging instrument was determined to be 0.93 ± 0.03 μm/pixel. Multispectral images of hydrogels in a 1 mm path length cell were recorded in the NIR region between 1400 and 2200 nm with 2 nm intervals.

A custom-built metal cell holder, equipped with six resistors and powered by the Tenna model PS-12 power supply, was used to study the effects of temperature on the hydrogel particles. A spectrophotometric cell was placed in the holder, and the temperature was precisely maintained by a RTD temperature controller (Athena Controls, Inc.; Model 4200-B-185). Typically, two initial measurements were taken at room temperature and then 25 °C. Subsequently, the temperature was raised in increments of 4 °C. To determine the actual temperature of the solution, a thermocouple was inserted directly into the cell containing the hydrogels.

Sample Preparation. Because water absorbs strongly in the NIR region (1400−2200 nm), aqueous hydrogel solutions were redispersed in deuterium oxide prior to analysis. This isotopic solvent exchange was accomplished by centrifuging an aliquot of

(15) Tran, C. D.; Cui, Y.; Smirnov, S. *Anal. Chem.* **1998**, *70*, 4701–4708.
(16) Fischer, M.; Tran, C. D. *Anal. Chem.* **1999**, *71*, 953–959.
(17) Fischer, M.; Tran, C. D. *Anal. Chem.* **1999**, *71*, 2255–2261.
(18) Khait, O.; Smirnov, S.; Tran, C. D. *Anal. Chem.* **2001**, *73*, 732–739.
(19) Tran, C. D.; Grishko, V. I.; Challa, S. *J. Phys. Chem. B* **2008**, *112*, 14548–14559.
(20) Mejac, I.; Bryan, W. W.; Lee, T. R.; Tran, C. D. *Anal. Chem.* **2009**, *81*, 6687–6694.
(21) Morris, M. D. *Microscopic and Spectroscopic Imaging of the Chemical State*; Marcel Dekker: New York, 1993.
(22) Kim, J. H.; Lee, T. R. *Chem. Mater.* **2004**, *16*, 3647–3651.
(23) Kim, J. H.; Lee, T. R. *Langmuir* **2007**, *23*, 6504–6509.

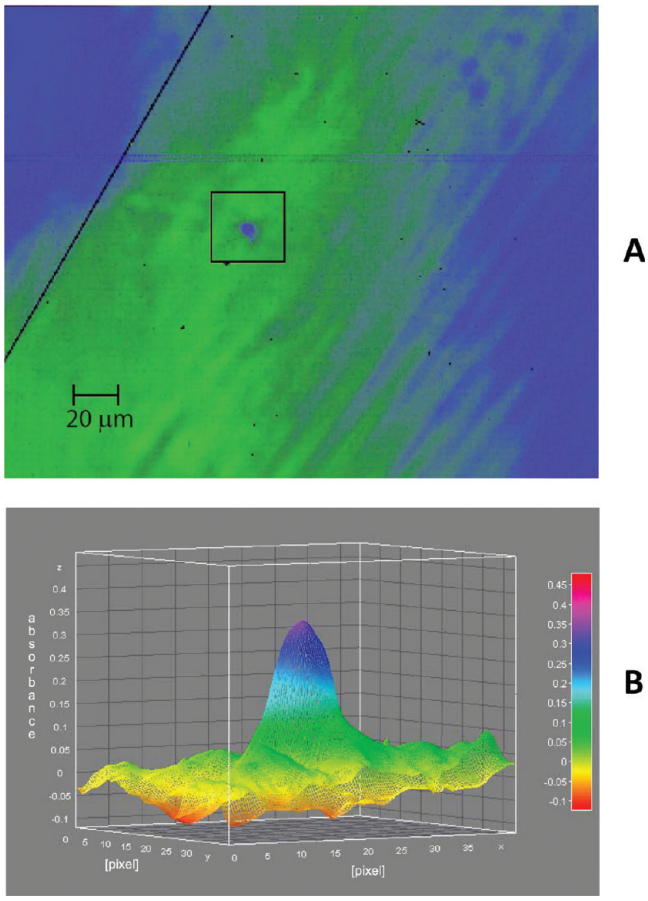

Figure 2. (A) 2-D image at 1764 nm of poly(NIPAM-*co*-AAc) hydrogel particle in D_2O and (B) corresponding 3-D absorption image of the drawn square section in (A). In the 2-D image, the hydrogel particle is blue, the background is green, and the black line in the upper left-hand corner is the marking of the NIR camera. Units for the *x*, *y*, and *z* axes of the 3-D image are pixel, pixel, and absorbance at 1764 nm, respectively.

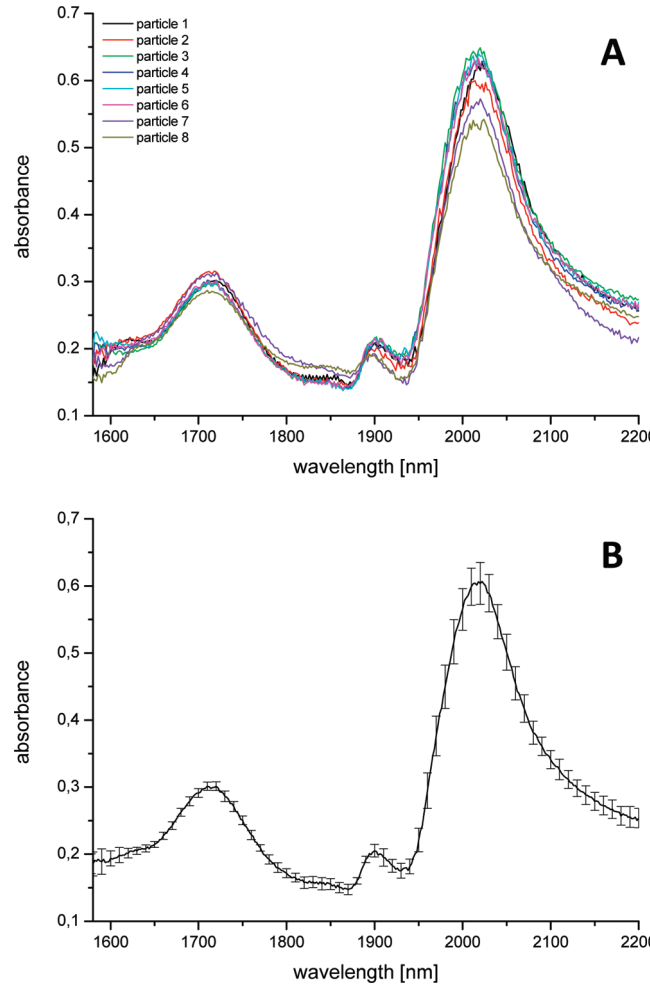

Figure 3. (A) Absorption spectra of eight different hydrogel particles in D_2O. (B) Average absorption spectrum of the hydrogel particles.

hydrogel solution in a 1.5 mL centrifuge tube at room temperature for 3 h at 5000 rpm. The aqueous supernatant was then discarded, and the hydrogel particles were redispersed in D_2O.

RESULTS AND DISCUSSION

As described above, the spatial resolution of the NIR-MSI microscope is 0.93 ± 0.03 μm/pixel. Given that the average diameter of the hydrogel particles used in this study are ≥1.0 μm (as determined by DLS), individual hydrogel particles can be observed and measured by the imaging instrument. Figure 2A shows a recorded (at 1764 nm) 2-D image of a hydrogel particle (where the hydrogel particle is dark blue, the background is green, and the black line is the NIR camera marking). A selected section of the 2-D image (Figure 2A) was taken to calculate a corresponding 3-D plot of the absorbance of a single hydrogel particle at 1764 nm (Figure 2B, where the units of *x*, *y*, and *z* axis are pixel, pixel, and absorbance, respectively). Finally, on the basis of the instrumental spatial resolution of 0.93 ± 0.03 μm/pixel and the images in Figure 2A,B, the diameter of the imaged hydrogel particle (in D_2O) was estimated to be 4.2 ± 0.5 μm. To characterize the particles further, NIR absorption spectra over the range of 1400 to 2200 nm of individual NIPAM-AAc hydrogels were extracted from their recorded images. One of the spectra shown in Figure 3A is that of a single particle whose image at 1764 nm is shown (in the square insert) in Figure 2A. Notably, this spectrum was extracted from recorded images using data from a single pixel. Furthermore, it is noteworthy that the S/N of the imaging instrument is excellent even at single-pixel scale. To evaluate the degree of chemical heterogeneity among the hydrogel particles, the NIR absorption spectra of seven additional hydrogel particles were individually collected. The spectra of all eight particles (see Figure 3A) are similar, which is consistent with no detectable chemical heterogeneity among the particles.

Figure 3B shows an averaged NIR spectrum of eight single particles together with their associated standard deviations. As illustrated, the difference between the NIR spectra of single particles is relatively small, less than 5% in all cases. As demonstrated by the spectra in this NIR region, the hydrogel particles exhibit two strong absorption bands at ~1714 and ~2016 nm. The former band can be attributed to C−H overtones and combination transitions,[24−30] while the latter is due to overtones of O−D

(24) Schmidt, P.; Dybal, J.; Trchova, M. *Vib. Spectrosc.* **2006**, *42*, 278–283.
(25) Sun, B.; Lin, Y.; Wu, P.; Siesler, H. W. *Macromolecules* **2008**, *41*, 1512–1520.
(26) Czarmecki, M. A.; Haufa, K. Z. *J. Phys. Chem. A* **2005**, *109*, 1015–1021.
(27) Langford, V. S.; McKinley, A. J.; Quckenden, T. I. *J. Phys. Chem A* **2001**, *105*, 8916–8921.

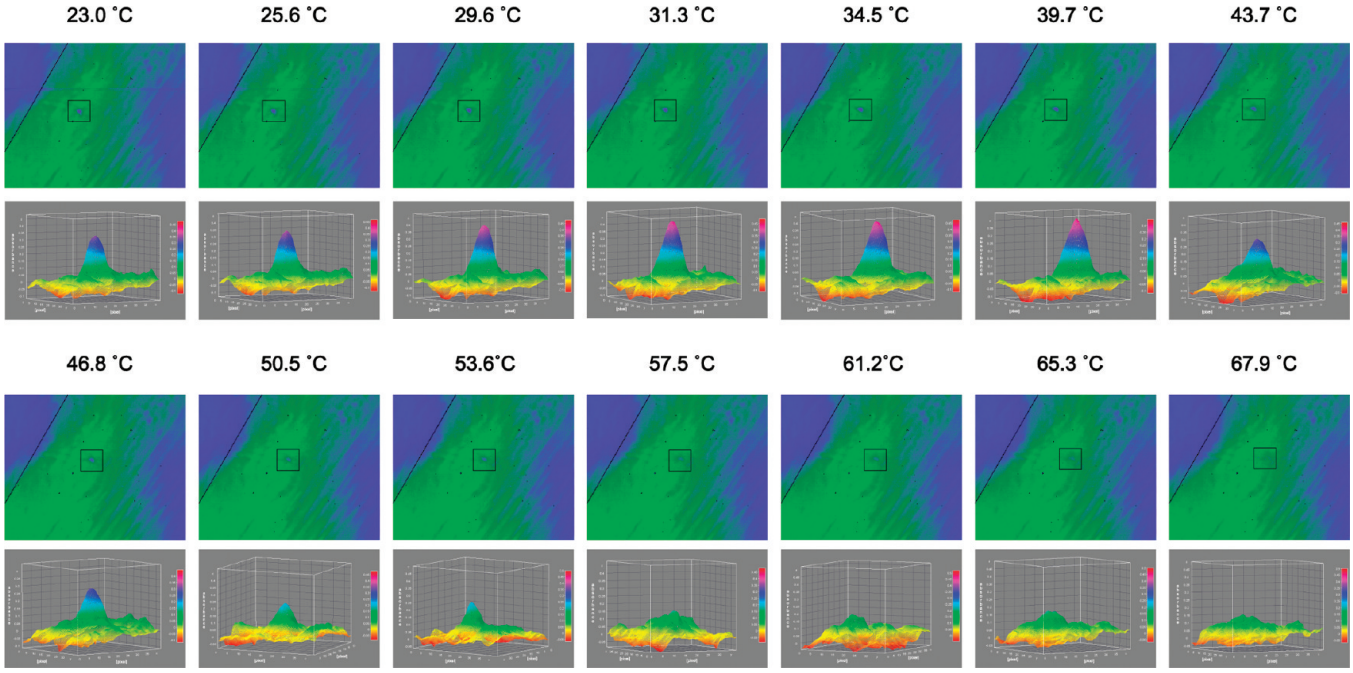

Figure 4. 2-D images and corresponding 3-D images of absorption at 1764 nm of the same single hydrogel particle at fourteen different temperatures: from 23.0 °C to gradually higher temperatures of 25.6, 29.6, 31.3, 34.5, 39.7, 43.7, 46.8, 50.5, 53.6, 57.5, 61.2, 65.3, and 67.9 °C (the fist 2-D and 3-D figures at 23.0 °C are the same as those shown in Figure 2). In the 2-D images, the hydrogel particle is blue, the background is green, and the black line in the upper left-hand corner is the marking of the NIR camera. Units for the *x*, *y*, and *z* axes of the 3-D images are the same as those in Figure 2B; that is, they are pixel, pixel, and absorbance at 1764 nm, respectively, where one pixel corresponds to 0.93 μm.

transitions in D_2O and in the carboxylic acid group of the hydrogels (through isotopic exchange with D_2O).[24−30]

As detailed in previous studies,[1−4] the size and chemical structure of hydrogels strongly depend on temperature. However, to date, this information was obtained not for a single hydrogel particle but rather for a collection of many different hydrogel particles in solution. It is, therefore, of particular interest to determine if a single hydrogel particle exhibits this behavior as well. Accordingly, we monitored and recorded NIR multispectral images of a single discrete hydrogel particle as a function of temperature, by heating the particle from room temperature to 67.9 °C and then cooling to 31.0 °C. The first and third rows of Figure 4 show 2-D images of the individual hydrogel particle recorded at 1764 nm (Figure 2A), heated from room temperature (23.0 °C) to increasing temperatures (25.6, 29.6, 31.3, 34.5, 39.7, 43.7, 46.8, 50.5, 53.6, 57.5, 61.2, 65.3, and 67.9 °C) before cooling the particle solution to 31.0 °C. As illustrated, the single hydrogel particle can clearly be observed from room temperature up to 53.6 °C. Thereafter, it is increasingly difficult to observe the particle, which vanishes completely upon reaching 61.2 °C and higher temperatures. Interestingly, the particle becomes visible again when allowed to cool from 67.9 to 31.0 °C (not shown).

The influence of temperature becomes more apparent when the 2-D images shown in the first and third rows of Figure 4 are plotted in 3-D as a function of absorbance at 1764 nm (i.e., the *z* axis is absorbance at 1764 nm). Corresponding 3-D images are shown in the second and fourth rows of Figure 4 (the first 2-D and 3-D images at 23.0 °C are the same as the images shown in Figure 2A,B, respectively). As illustrated, when the temperature of the sample reaches 43.7 °C, a decrease in NIR absorption intensity occurs, and any additional heating leads to a further decrease. Importantly, the sample recovers its absorption intensity when cooled from 67.9 to 31.0 °C. Because the 2-D and 3-D images were taken at 1764 nm, the results presented here suggest that heating the hydrogel particle has a combined effect of lowering its absorption at 1764 nm and reducing its size to dimensions too small to be measured using our NIR-MSI microscope (i.e., smaller than 0.9 μm). Additional studies of the effects of temperature on a single hydrogel particle over the entire NIR spectral region from 1400 and 2200 nm (in contrast to a single wavelength of 1764 nm) can help to resolve this issue.

Figure 5A shows the absorption spectra (which were extracted from recorded images using data from a single pixel) of a single hydrogel particle (shown in Figure 4) as a function of increasing temperature. Clearly, increasing the temperature has a pronounced effect on the spectra of the hydrogel, particularly for the bands at ~1714 and ~1898 nm. Interestingly, increasing the temperature not only lowers the absorption intensity but also produces a blue-shift of the 1714 nm band, which arises from C−H overtones and combination transitions.[24−30] Conversely, a substantial increase in the 1898 nm band was also observed with increasing temperature. This trend becomes more apparent in Figure 5B, which shows only three of the 13 spectra: spectra at 23.0 °C (black curve), at 65.3 °C (red curve), and after the heated hydrogel was allowed to cool back down to 31.0 °C (green curve). It is evident that raising the temperature leads to a lower absorbance as well as blue-shifting of the C−H band from 1714 to 1706 nm.

(28) Waggener, W. C. *Anal. Chem.* **1956**, *30*, 1569–1570.
(29) Harvey, D. K.; Feierabend, K. J.; Black, J. C.; Vaida, V. *J. Mol. Spectrosc.* **2005**, *229*, 151–157.
(30) Geuken, B.; Meersman, F.; Nies, E. *J. Phys. Chem. B* **2008**, *112*, 4474–4477.

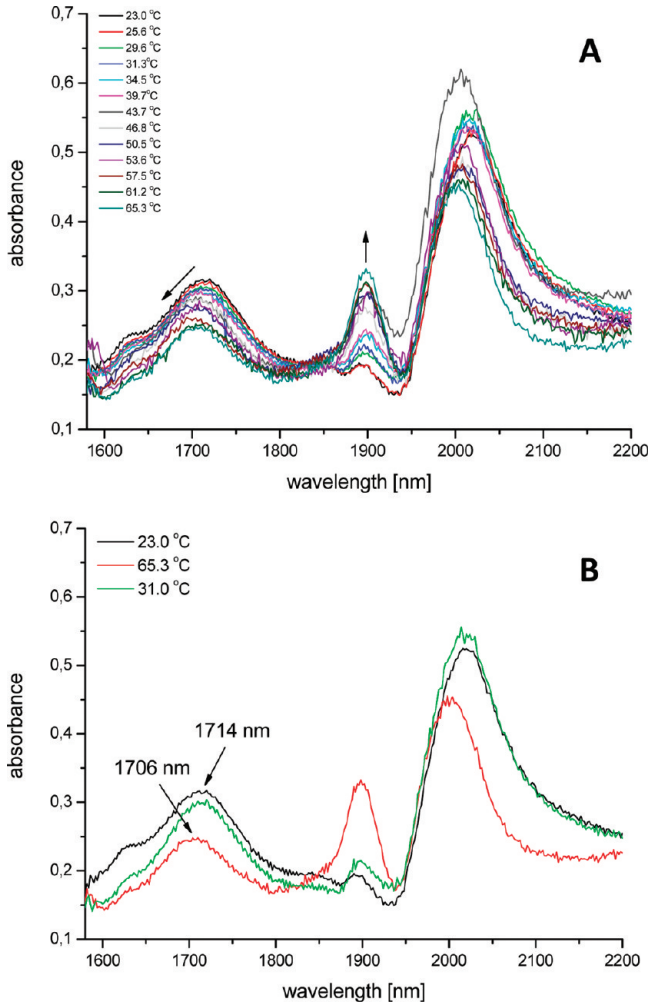

Figure 5. (A) Absorption spectra of a single hydrogel particle in D_2O at different temperatures. (B) Comparison of the absorption spectra at final and initial temperatures.

Particularly interesting is the reversibility of the absorption and the return of the λ_{max} to its original position at 1714 nm as the single hydrogel particles were cooled to 31.0 °C.

Additional experiments were performed to gain insight into the relationship between temperature and the increased absorbance of the band at 1898 nm. It should be reemphasized that the hydrogel particles used in this study were poly(NIPAM-*co*-AAc), 95:5 w/w. As such, a sample of the hydrogel particles in D_2O can, therefore, be considered chemically similar to a 95:5 w/w mixture of acetamide/acetic acid in D_2O. Accordingly, temperature effects on the absorption spectra of neat acetic acid, acetamide in D_2O, and neat D_2O were investigated (spectra not shown). The spectra shown in Figure S1 in the Supporting Information are difference spectra, obtained by subtracting the spectra obtained at room temperature (23.0 °C) from the spectra of the same solution heated to 65.3 °C for (A) D_2O, (B) acetamide in D_2O, (C) neat acetic acid, and (D) combined difference spectra of (i) a single hydrogel particle in D_2O (green curve), (ii) acetamide in D_2O (red curve), and (iii) a 95:5 w/w mixture of acetamide/acetic acid in D_2O (black curve). A pronounced band at ~1890 nm can be observed in the difference spectra of D_2O and acetamide in D_2O (Figure S1A,B in the Supporting Information), contrasting that of acetic acid (Figure S1C in the Supporting Information). The three spectra shown in Figure S1D (in the Supporting Information) are similar; however, upon closer examination, the spectrum of the 95:5 w/w mixture of acetamide/acetic acid in D_2O (black curve) more closely resembles that of the hydrogel (green curve) than that of acetamide in D_2O (red curve). As a whole, the results are consistent with previous studies[14−30] suggesting that the 1898 nm band corresponds to the hot band of the O−D groups (from D_2O, from the hydrogel particle, and from the 95:5 w/w mixture of acetamide/acetic acid in D_2O).

Additional structural information regarding the hydrogels and their response to temperature can be obtained by carefully inspecting the spectra in Figure 5A. Figure 6A shows a plot of change in the λ_{max} positions of the 1714 nm band as a function of temperature and the best fit curve to experimental data (detailed information on the best fit curve is shown in Figure S2A in the Supporting Information). As illustrated, it is evident that no significant changes in the λ_{max} positions occur from room temperature to 30 °C. However, as the temperature increases further, a substantial decrease in the value of λ_{max} is observed. Increasing the temperature beyond 45 °C yields a constant λ_{max} position, which suggests that the hydrogel undergoes a transition at a temperature. The exact phase transition temperature, determined by taking the second derivative of the best fit curve (plot of the first and second derivative curves is shown in Figure S2B in the Supporting Information), was found to be (41 ± 2 °C). The observed transition of this C−H band might be due, in part, to the fact that upon heating, the hydrogel moieties lose their sphere of hydration, which leads to an increase in the attractive interactions among the polymer chains (which is reflected by a blue shift of the C−H band). This phenomenon corresponds to the known collapse of the hydrogel network, which leads to a reduction in size.[1−4] Furthermore, the process is thermally reversible: upon cooling, rehydration of the hydrogel occurs, reverting the particle to its original size (and red-shifting the λ_{max} to its original position).[24,25]

Alternatively, the volume transition temperature of the hydrogel particle can be obtained by plotting normalized changes in total absorption of the hydrogel (i.e., the area under the absorption spectrum for each temperature shown in Figure 5A) between two consecutive temperatures. Figure 6B plots the change in total absorption as a function of temperature for a single hydrogel particle (red data points) and also for the 95:5 w/w acetamide/acetic acid mixture in D_2O (black data points) together with the best fit to a Lorentzian curve. Consequently, the hydrogel undergoes a clear transition at 44 ± 2 °C (determined by taking the second derivative of the best fit curve (plot is shown in Figure S3B in the Supporting Information). This value is consistent with the transition temperature obtained from the plot of λ_{max} vs temperature (Figure 6A). Additionally, the absence of transitions when analyzing chemically similar mixtures of acetamide/acetic acid in D_2O further confirms that the observed transition is indeed specific to the hydrogel. As noted above, the observation of these transitions can be understood based on the polymeric nature of hydrogel polymers, which undergo reversible dehydration upon heating, leading to substantial reductions in size/volume.[1−4] This behavior contrasts that of

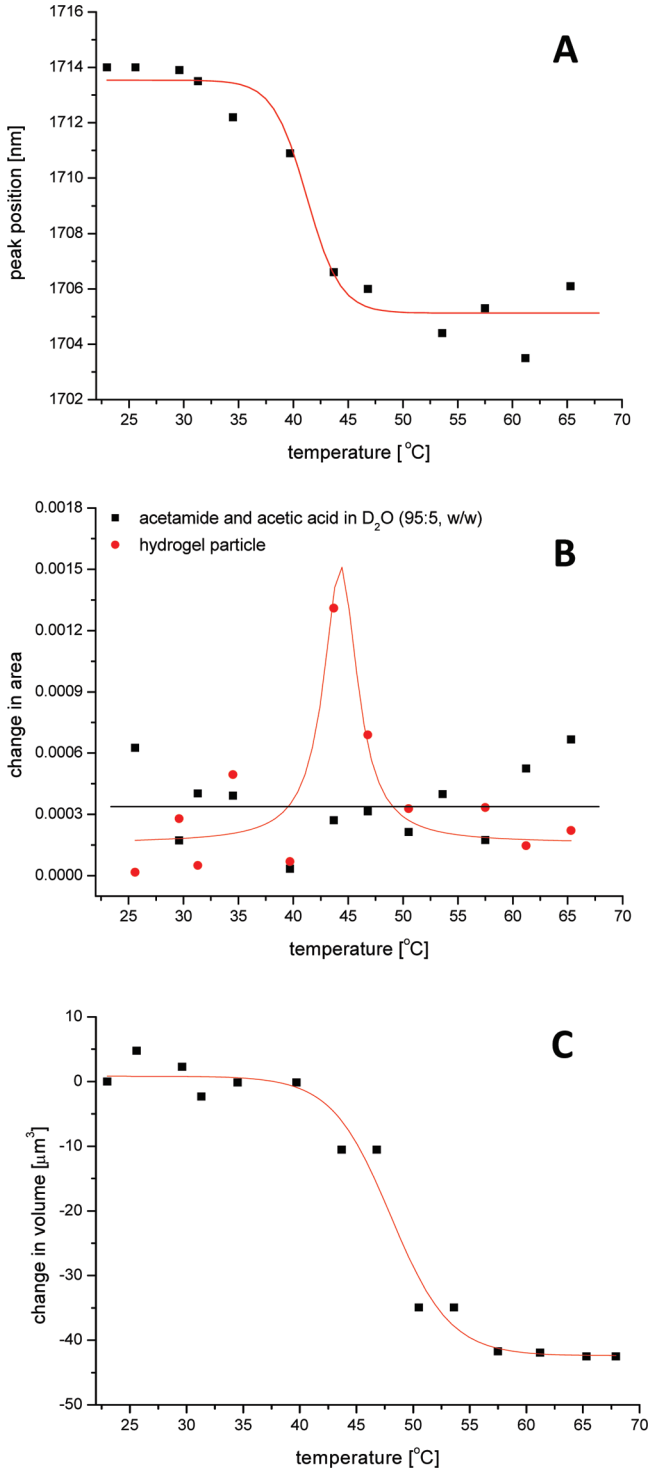

Figure 6. Plots of (A) λ_{max} of the C−H band, (B) change in area under spectra, and (C) change in volume of the same single hydrogel particle (relative to its volume of 42.9 μm^3 at 23 °C) as a function of temperature. See text for detailed description.

nonpolymeric acetamide/acetic acid mixtures, which plausibly lack transitions of this type.

Rather than indirectly determining the volume transition temperature of individual hydrogel particles from plots of either λ_{max} or absorbance vs temperature, as described above, the volume transition temperature of the hydrogel can be determined directly by plotting the change in the hydrogel volume as a function of temperature. This result is possible because each individual hydrogel particle can be observed by the NIR-MSI microscope. Consequently, from the recorded images at different temperatures shown in Figure 4, the volume of a single hydrogel particle at different temperatures was calculated. Figure 6C shows a plot of changes in volume of a single hydrogel particle (relative to its volume of 42.9 μm^3 at 23 °C) as a function of temperature. As illustrated, rapid changes in hydrogel volume were observed in the temperatures from 40−55 °C. Little or no changes in volume occur above or below this range of temperatures. The volume transition temperature of the hydrogel particle, determined from the second derivative of the best fit curve (plot shown in Figure S4B in the Supporting Information), was found to be 48 ± 3 °C.

As discussed above, increasing temperature leads to shift in λ_{max} (toward shorter wavelength) and decrease in absorbance of the hydrogel particle. However, such wavelength shift and absorbance change do not contribute to the observed volume changes presented in Figure 6C even though volumes of the particle were calculated from its images recorded at 1764 nm. This is due to the fact that changes in absorbance of the particle as function of temperature is linear and much smaller than changes in volume; e.g., absorbance at 1764 nm is 0.248 and 0.196 at 23 and 61.2 °C, respectively. This is not surprising considering the fact that the band around 1764 nm is due not to O−D but to C−H overtones and combination transitions. The particle disappears at around 61.2 °C (Figure 4) because at this temperature the size of the particle is too small to be observed by the microscope (i.e., smaller than spatial resolution of the microscope). Since, at this temperature, the hydrogel particle still exhibits an absorbance of 0.196, it would have been observed if its size were larger than the spatial resolution of the microscope. In fact, volumes of the same hydrogel particle (at a given temperature) were found to be the same when determined from images recorded at several different wavelengths where a difference in their absorbance is larger than 0.058 which is for 1764 nm at 23 and 65.3 °C.

To evaluate the size-dependency of the LCST, individual hydrogel particles of varying sizes were prepared in several batches by slightly adjusting the pH of the solution. Six different discrete hydrogel particles with sizes ranging from 1.2 ± 0.4 to 5.9 ± 0.5 μm were selected, and their LCST values were determined. Because each individual hydrogel particle can be directly observed, it was possible to rule out the existence of any dimers or aggregated particles. As such, the LCST values obtained for these hydrogels were plotted as a function of their volume (Figure 7). As illustrated, the LCST values are strongly dependent on their size. Smaller hydrogels were found to have lower LCST values (e.g., the 1.2 ± 0.4 μm sized hydrogel particle has an LCST value of 35.0 °C, and the 5.9 ± 0.5 μm sized hydrogel particle has an LCST value of 61 °C); correspondingly, the LCST value for the hydrogels with intermediate sizes fell in between those extremes (e.g., the 3.1 ± 0.4 and 3.3 ± 0.5 μm hydrogel particles have LCST values of 44 and 42 °C, respectively). Considering the fact that the LCST corresponds to dehydration of hydrogel particles, this finding, albeit unprecedented, is plausible given that smaller hydrogel particles have relatively fewer hydrated sites and thus undergo dehydration more readily than larger hydrogel particles.

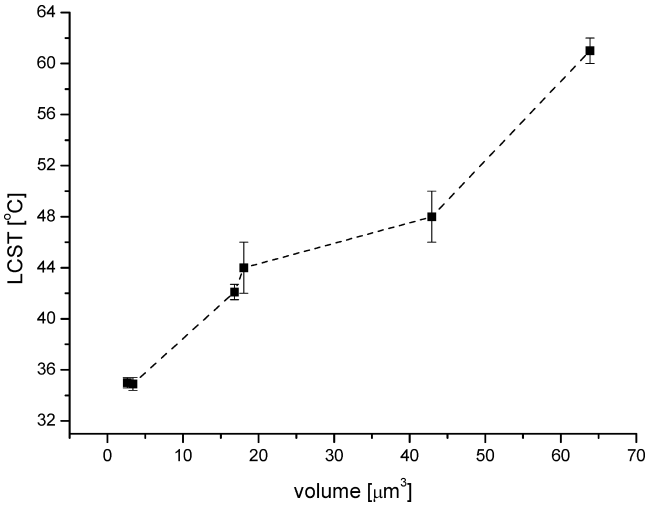

Figure 7. Plot of LCST value as a function of volume for individual hydrogel particles.

As a whole, the newly developed NIR-MSI microscope makes it possible, for the first time, to observe and characterize directly individual hydrogel particles in solution. Moreover, on the basis of the use of this microscope, three different methods can be utilized for the determination of the volume transition temperature of a single hydrogel particle. Importantly, the transition temperatures obtained by these methods are not only self-consistent but also consistent with the LCST values obtained by other methods, including dynamic light scattering. The consistency of these data further confirms the accuracy and reliability of our new analytical method. It is further important to note that the methods reported here are based on direct observation and determination of the LCST values of discrete hydrogel particles, whereas all LCST values previously reported are based on measurements not of a single hydrogel particle but rather of a collection of many hydrogel particles. Due to this advantage, the methods reported here can be used, for the first time, to determine if any factor (e.g., particle size) influences the LCST values of individual hydrogel particles.

CONCLUSIONS

We have demonstrated for the first time that the NIR-MSI microscope can be successfully used to observe and measure directly images and spectra of individual hydrogel particles. Because both images and spectra of the individual particles can be directly and simultaneously measured by the microscope, it is possible to detect any changes in the spectroscopic properties and/or nature (size, volume) of individual hydrogel particles that can be induced by external factors (e.g., temperature and/or pH). These features make possible the development of three unique methods for determining LCST values based on monitoring either changes in the NIR spectra or the volume of the hydrogel particle in response to variations in temperature. For the first time, a unique means to measure the volume transition temperature or LCST value, not of a collection of many hydrogel particles, but rather of individual hydrogel particles, is made possible. Using such methods, we find that the LCST of individual hydrogel particles depends on the particle size, with larger particles exhibiting higher LCST values.

ACKNOWLEDGMENT

The National Science Foundation (ECCS-0926027) and the Texas Center for Superconductivity provided generous support for the work at the University of Houston.

SUPPORTING INFORMATION AVAILABLE

Additional information as noted in text. This material is available free of charge via the Internet at http://pubs.acs.org.

Received for review September 18, 2009. Accepted January 17, 2010.

AC902099D